[18F]DOPA PET identifies metabolically active tumor beyond contrast-enhancing margins in IDH-WT glioblastoma: a histopathology and fluorescence validation study

[^{18}F]DOPA PET identifies metabolically active tumor beyond contrast-enhancing margins in IDH-WT glioblastoma: a histopathology and fluorescence validation study

Andrea Bianconi[1,2], Alessandro Pesaresi[3], Raffaele De Marco[3], Michela Zotta[4], Luca Bertero[5], Francesco Bruno[6], Edoardo Pronello[6], Giulia Capella[5], Flavio Panico[3], Adriana Lesca[4], Fabio Cofano[3], Paola Cassoni[5], Giovanni Morana[7], Roberta Rudà[6], Silvia Morbelli[4,8], Diego Garbossa[3]

Affiliations:

[1] Department of Neuroscience, Rehabilitation, Ophthalmology, Genetics, Maternal and Child Health (DINOGMI), University of Genova, 16132 Genova, Italy

[2] Neurosurgery Unit, IRCCS Ospedale Policlinico San Martino, Genova, 16132, Genova, Italy

[3] Neurosurgery Unit, Department of Neuroscience, University of Turin, Turin, Italy

[4] Nuclear Medicine Unit, AOU Città Della Salute e Della Scienza di Torino, Turin, Italy

[5] Pathology Unit, Dept. Medical Sciences, University of Turin, Turin, Italy.

[6] Division of Neuro-Oncology, Department of Neuroscience, University and City of Health and Science Hospital, Turin, Italy

[7] Division of Neuroradiology, Department of Diagnostic Imaging and Radiotherapy, "Città della Salute e della Scienza" University Hospital, University of Turin, 10124 Turin, Italy

[8] Department of Medical Sciences, University of Turin, Turin, Italy.

Running title: [^{18}F]DOPA PET validation for supramaximal resection in GB

Correspondence:

Andrea Bianconi, MD,

Department of Neuroscience, Rehabilitation, Ophthalmology, Genetics, Maternal and Child Health (DINOGMI), University of Genova,

Largo Paolo Daneo 3,

16132 Genova, Italy

Email: andrea.bianconi@unige.it

Andrea Bianconi and Alessandro Pesaresi contributed equally to this work.

Word count: 3416

Abstract

Background: Supramaximal resection in IDH-wildtype glioblastoma (GB) improves survival, yet identifying tumor infiltration within FLAIR-hyperintense peritumoral areas remains challenging. This study aims to validate the use of [^{18}F]DOPA PET for identifying metabolically active tumor beyond Contrast enhancing (CE) margins, correlating imaging with histopathology and intraoperative fluorescence.

Methods: Patients with newly diagnosed IDH-wt GB scheduled for supramaximal resection and undergoing preoperative DOPA-PET and MRI were prospectively enrolled from the ResPGlioma study. The Biological Tumor Volume (BTV) was semi-automatically delineated using the contralateral striatal SUVmean as the PET positivity threshold. Before resection, biopsy samples were collected from five radiologically distinct areas: CE, FLAIR+PET (FP), PET-only (Po), FLAIR-only (Fo), and normal tissue (N). Each sample was blindly assessed for neoplastic, necrotic, and infiltrative components, mitotic count, microvascular proliferation. Intraoperative 5-aminolevulinic acid (5-ALA) and fluorescein sodium (FS) uptake were also recorded.

Results: Twenty-five samples from 5 patients were analyzed. The BTV, defined using a striatal SUVmean threshold, extended beyond CE-MRI margins in 100% of cases (mean BTV 30.4 ± 17.6 cm³ vs. mean CE volume 20.6 ± 16.9 cm³). PET-positive areas (FLAIR+/PET+ and PET-only) showed significantly higher neoplastic cell density and mitotic counts compared to FLAIR-only ($p<0.005$) and normal areas ($p<0.005$). No significant histopathological differences were found between PET-only and CE regions, whereas FLAIR-only samples primarily exhibited white matter infiltration and reactive changes. Uptake of 5-ALA and SF was significantly more intense and frequent in PET-positive areas (CE, FP, Po) compared to Fo and N areas ($p=0.015$ and $p<0.001$, respectively).

Conclusions: This preliminary study provides histopathological and fluorescence validation that [^{18}F]DOPA PET identifies areas of high tumor burden within the peritumoral zone, comparable to the contrast-enhancing core. The integration of amino acid PET in preoperative planning should be considered to guide targeted supramaximal resection of metabolic hotspots in IDH-wildtype glioblastoma.

Key words:

1 [18F]-DOPA PET

2 Glioblastoma, IDH-wildtype

3 5-aminolevulinic acid

4 Amino acid PET

5 Supramaximal resection

Key points:

1 [18F] DOPA PET identifies high-density tumor infiltration beyond contrast enhancement.

2 5-ALA correlates with [18F] DOPA PET-positive areas, while fluorescein confirms blood-brain barrier disruption, predominantly in CE regions.

3 [18F] DOPA PET-guided resection may enable safer supramaximal resection by targeting metabolically active tumor outside CE areas.

Importance of the study

Achieving supramaximal resection in glioblastoma is often limited by conventional MRI inability to distinguish high-burden tumor infiltration from reactive edema within FLAIR-hyperintense regions. In this interim analysis from the ongoing ResPGlioma study, we provide blinded histopathological validation and intraoperative fluorescence correlation (5-ALA and Fluorescein Sodium). Our preliminary results demonstrate that [18F]DOPA PET/CT identifies metabolically active areas beyond contrast-enhancing margins that harbor mitotic activity and neoplastic cell densities comparable to the tumor core, while FLAIR-only areas show predominantly reactive changes. Furthermore, 5-ALA fluorescence closely mirrors metabolic

PET-positivity, while fluorescein confirms blood-brain barrier disruption. These findings support integrating amino acid PET into surgical planning to optimize maximal safe resection by targeting metabolic tumor "hotspots" rather than resecting the entire FLAIR-hyperintense area.

INTRODUCTION

Surgical resection is the cornerstone of therapy for IDH-wildtype glioblastoma (GB). While resecting >98% of the contrast-enhancing (CE) tumor improves survival, the latest RANO classification shows that supramaximal resection (Class 1: complete CE removal plus ≤5 cm^3 non-CE tumor) yields better outcomes.[1] The infiltrative nature of gliomas often leads to tumor recurrence beyond the margins of the contrast-enhancing nodule. Regions outside these margins contain a significant number of tumor cells, which may account for the high recurrence rates.[2,3] Indeed, extending surgical resection beyond the CE area, such as by resecting Fluid-Attenuated Inversion Recovery (FLAIR) hyperintensities at Magnetic Resonance Imaging (MRI), can improve Overall Survival (OS). [4,5] Fluorescence-guided surgery (FGS), particularly with 5-aminolevulinic acid (5-ALA) and fluorescein sodium (FS), is one of the tools used to achieve supramaximal resection by identifying peritumoral regions with high metabolic activity.[6–8] However, in clinical practice, it can be challenging to resect a broad area like the FLAIR hyperintense region, especially near eloquent areas.[9] In such cases, a supratotal resection may severely compromise functional outcomes, impacting not only quality of life but also subsequent therapeutic options and, ultimately, survival. For these reasons, although the benefits of supramaximal resection in GB are widely acknowledged, there remains debate about how far surgeons should extend resection beyond the CE area.[10]

In recent years, resection guided by brain positron emission tomography/computed tomography (PET/CT) with radiopharmaceuticals for amino acids uptake (AA-PET) has emerged as a promising alternative for achieving maximal safe resection in patients with GB.[11,12] Furthermore, areas of increased uptake on AA-PET correlates with regions of higher metabolic activity at MR spectroscopy, demonstrating greater specificity than FLAIR MRI in detecting GB cells beyond the CE area. [13,14] Thus, AA-PET-guided resection could facilitate an increase in extent of resection

(EOR) beyond the CE margin, improving OS and progression-free survival (PFS) while reducing the risk of damaging adjacent functional areas that are not involved in the disease.[15]

The purpose of this preliminary histopathological validation study is to investigate the specificity of AA-PET/CT with [^{18}F]DOPA (DOPA PET) in quantifying glioma cells in comparison to reactive healthy tissue, differentiating it from contrast-enhanced areas and, even more, from the FLAIR abnormality area outside the CE borders. Secondarily, the uptake of the fluorophores (5-ALA and FS) in the tumoral and peritumoral areas was evaluated.

METHODS

Adult patients (age >18 years) with a suspected newly diagnosed IDH-wildtype glioblastoma based on preoperative MRI were prospectively enrolled in the ResPGlioma study (Institutional Review Board (IRB) n. 698050/2023, ClinicalTrials.gov identifier: NCT07567196). Specifically, lesions with a high radiological suspicion of glioblastoma at MRI were selected for preoperative DOPA PET, which was conducted within one week prior to surgery. The final diagnosis of IDH-wildtype glioblastoma was subsequently confirmed by postoperative histopathology according to the WHO 2021 classification.

Patients with conditions that contraindicated the execution of DOPA PET (e.g., pregnancy or breastfeeding), those with 3 Tesla (3T) MRI compatibility issues (e.g., pacemakers or defibrillators), or individuals from whom informed consent could not be obtained were excluded from the study.

The present analysis is a predefined secondary endpoint of the ResPGlioma study (NCT07567196). The study protocol, including inclusion/exclusion criteria, primary and secondary endpoints, and outcome measures, is provided as Supplementary File 1. For this specific study, a subset of patients from the ResPGlioma study was included. Only patients whose tumor reached the cortical surface were selected, in order to avoid the brainshift phenomenon and the resulting loss of accuracy of the neuronavigation system during biopsies. Similarly, only patients with isolated (unifocal) tumors and a preoperative plan for supramaximal resection were included, to allow for biopsy sampling in all the considered peritumoral areas. (Fig.1)

[^{18}F]-DOPA-PET/CT and MRI Imaging Protocol

DOPA PET data acquisition was performed on a Philips Vereos digital hybrid PET/CT following EANM/EANO guidelines[16]. Briefly, patients fasted for at least 4 hours before administration of about 2MBq/kg of DOPA (fluorodopa (18F), Curium, Italy). Premedication with Carbidopa was not carried out. Images were acquired approximately 15-20 minutes after the injection, with a scanning time of 20 minutes (one static image reconstructed using an OSEM 3D algorithm: 2 iterations, 10 subsets, $256 \times 256 \times 164$ voxels, no post-filtering). A non-diagnostic low dose CT scan was used for attenuation correction.

The biological tumor volume (BTV) was defined based on the mean standard uptake value of the contralateral striatum.[17] The striatum was delineated on the F-DOPA PET images by placing a specific region of interest (ROI) over the contralateral healthy striatum to calculate the mean Standardized Uptake Value (SUVmean). BTV quantification was semi-automatically performed in three dimensions using a dedicated workstation (Mirada software, Philips HealthCare) as

previously detailed.[18] A 2D ROI was preferred over a 3D VOI for striatal SUVmean computation. This approach allows reliable sampling of the striatal uptake peak while minimizing contamination from surrounding structures with lower physiological [^{18}F]DOPA uptake. Measures were assessed jointly by two Nuclear Medicine physicians (MZ and AL). In cases of disagreement, final classification was established through consensus discussion among the two observers.

DOPA PET was then coregistered with MRI sequences of interest, specifically contrast-enhanced T1-weighted images (to identify the CE volume, Figure 1a) and T2-weighted FLAIR sequences (to delineate hyperintensities outside the CE areas, Figure 1b). If the MRI was more than two weeks older than the scheduled date of surgery, it was repeated. MRI examinations were acquired using a 3T scanner (Ingenia, Philips, Best, the Netherlands). Imaging co-registration and volume segmentation were performed semi-automatically using iPlan software from BrainLab AG, Munich, Germany. Semi-automated segmentation was performed by two neurosurgeons (RDM and AP) independently; any disagreements were resolved through discussion to reach consensus. The final segmentations were then reviewed and approved by a senior neurosurgeon (DG) and a neuroradiologist (GM). Volume measurements (CE volume, PET volume, and FLAIR volume) all included the entire necrotic core.

Following co-registration and segmentation, the fused PET/MRI dataset was transferred to the BrainLab neuronavigation system and used intraoperatively for real-time surgical guidance during biopsy sampling and resection.

Surgical Procedure

All procedures were conducted at a single institution in 2023 after IRB approval. Both 5-ALA and SF were administered in each procedure, as described in the previous articles[6,19]. Intraoperative

neuromonitoring (IONM) for motor evoked potentials (MEPs), somatosensory evoked potentials (SSEPs), and cortical and subcortical stimulation was utilized in all cases.

To enhance the accuracy of biopsies and minimize the influence of "brain shift", the selected areas for planned biopsies were accessed prior to tumor resection. A small corticectomy was planned at a location that allowed access to the various sampling areas.

Five different areas were considered to collect samples (Figure 1 and 2):

- CE: CE areas.
- FP: FLAIR+PET areas.
- Po: PET-only areas.
- Fo: FLAIR-only areas.
- N: areas with no evident PET/MRI disease.

Patients were excluded if biopsies of all areas could not be obtained with sufficient accuracy due to tumor location, functional constraints, or if any of the areas were not clearly identifiable on imaging . The intensity of 5-ALA and FS uptake was initially assessed jointly by two neurosurgeons present during the surgery and categorized as either “intense”, “faint” or negative (14). A third independent observer, blinded to the sampling areas, retrospectively reviewed the surgical videos and performed the same classification. Interobserver agreement between the initial joint classification and the blinded evaluation was assessed using Cohen’s kappa coefficient. In cases of disagreement, final classification was established through consensus discussion among all three observers.

Histopathological Evaluation

An experienced pathologist blindly evaluated these samples defining the amount of: 1) neoplastic component (%), 2) necrosis (%), 3) mitotic count in/10 high power fields, (HPF, 400X); 4) vascular proliferations (absent, focal or diffuse), 5) infiltrative component (%) and 6) normal/reactive component (%). Morphological features were assessed on routinely processed hematoxylin-eosin histological slides. Samples without parenchymal areas were excluded. To address the potential subjective evaluation biases, samples were simultaneously evaluated by two pathologists (LB and PC) and a consensus agreement achieved. (Figure 3)

Statistical Analysis

Descriptive statistics are reported as the mean and standard deviation for continuous variables and as frequency and percentage for nominal variables. The Shapiro-Wilk test was performed to assess the normality assumption of the data. The Levene's test was conducted to evaluate the equality of variances. Differences between multiple groups were assessed using a one-way parametric ANOVA, according to the assumptions met. Differences between two groups were evaluated using the Mann-Whitney U test for independent samples, according to the assumptions met. The chi-square (χ^2) test was used to assess associations between nominal variables. A p-value < 0.05 was considered statistically significant. All the statistical analysis was conducted using an open-source software built on R language (The jamovi project (2021)". jamovi. (Version 2.2) [Computer Software]. Retrieved from https://www.jamovi.org). Statistical significance was set at $p \leq 0.05$.

RESULTS

The pathological validation was performed on 25 samples collected from 5 patients (3 females and 2 males). The mean age was 68.4 ± 8.8 years (range: 56-71 years), with a mean preoperative Karnofsky Performance Status (KPS) of 92 ± 4.5 (range: 90-100). The temporal lobe was affected in 3 cases (60%), while the tumor was located in the frontal lobe in the remaining 2 cases (40%). In 4 cases, GB was localized to the non-dominant hemisphere (80%).

The mean volume of CE-T1w was 20.6 ± 16.9 cm^3 (range: 1.55-44.6 cm^3), the mean DOPA PET/CT volume was 30.4 ± 17.6 cm^3 (range: 4.73-47.1 cm^3), and the mean FLAIR volume was 60.1 ± 62.0 cm^3 (range: 5.35-165 cm^3).

All patient data are reported in Table 1.

Correlation between the Sample Collection Area and Histopathological Examination

Considering histopathological characteristics, we observed differences among the groups. Table 2 shows the histopathological variables evaluated across the different samples. (Table 2).

Neoplastic Component

The highest values of the neoplastic component were observed in the CE samples (mean: 92.00±8.37%, range: 80-100%), FLAIR+PET (mean: 82.00±24.90%, range: 40-100%), and PET-only (mean: 78.00±27.75%, range: 30-100%). The lowest values were observed in the FLAIR-only samples (mean: 21.00±17.46%, range: 0-40%) and in the radiologically normal areas (mean: 9.00±17.46%, range: 0-40%). Statistically significant differences were observed when comparing the CE, FLAIR+PET, and PET-only areas with the FLAIR-only area ($p<0.001$, $p=0.002$, and $p=0.002$, respectively), as well as between these areas and the radiologically normal regions

($p<0.001$, $p<0.001$, and $p=0.002$, respectively). No statistically significant differences were observed between the CE, FLAIR+PET, and PET-only areas ($p>0.05$), nor between the FLAIR-only and radiologically normal areas ($p>0.05$) (Figure 4a).

Necrotic Component

The samples taken from the CE area exhibited the highest values of the necrotic component (mean: 25.00±13.23%, range: 5-40%). Statistically significant differences were found between the necrotic component in the CE area and the PET-only (mean: 6.00±6.52%, range: 0-15%, $p=0.020$), FLAIR-only (mean: 6.00±6.52%, range: 0-5%, $p=0.004$), and radiologically normal areas (mean: 6.00±5.48%, range: 0-10%, $p=0.018$). No significant differences were observed between the CE area and the FLAIR+PET area (mean: 11.00±13.42%, range: 0-30%, $p>0.05$). Furthermore, no statistically significant differences were found when comparing the FLAIR+PET, PET-only, FLAIR-only, and radiologically normal areas ($p>0.05$) (Figure 4b).

Mitoses

The highest mitotic count values were observed in the CE samples (mean: 22.60±14.64/10HPF, range: 9-41/10HPF), FLAIR+PET (mean: 18.40±8.14/10HPF, range: 7-30/10HPF), and PET-only (mean: 22.80±19.52/10HPF, range: 8-54/10HPF). The lowest values were found in the FLAIR-only samples (mean: 5.20±3.90/10HPF, range: 0-10/10HPF) and the radiologically normal areas (mean: 1.60±2.07/10HPF, range: 0-5/10HPF).

When comparing the samples, statistically significant differences were observed between the CE, FLAIR+PET, and PET-only areas and the FLAIR-only area ($p=0.033$, $p=0.011$, and $p=0.035$, respectively), as well as between these areas and the radiologically normal regions ($p=0.013$,

p=0.002, and p=0.012, respectively). No significant differences were observed between the CE, FLAIR+PET, and PET-only areas (p>0.05), nor between the FLAIR-only and radiologically normal areas (p>0.05) (Figure 4c).

Infiltrative Component

The samples taken from the FLAIR-only area exhibited the highest white matter infiltration (mean: 54.00±35.07%, range: 0-90%), compared to the samples obtained from the CE area (mean: 8.00±8.37%, range: 0-20%, p=0.021), FLAIR+PET (mean: 16.00±20.74%, range: 0-50%, p=0.037), and PET-only (mean: 18.00±19.24%, range: 0-50%, p=0.042). No significant differences were observed when comparing these areas with the samples from the radiologically normal area (mean: 22.00±25.88%, range: 0-50%, p>0.05). No statistically significant differences were found when comparing the CE, FLAIR+PET, PET-only, and radiologically normal areas (p>0.05) (Figure 4d).

Normal/Reactive Component

The samples taken from the radiologically normal areas showed the highest values of the normal/reactive component (mean: 63.00±44.10%, range: 10-100%). Normal/reactive components were also observed in the samples from the CE area. Statistically significant differences were found between the radiologically normal area and the CE (p=0.007), FLAIR+PET (mean: 2.00±4.47%, range: 0-10%, p=0.013), and PET-only areas (mean: 4.00±8.94%, range: 0-20%, p=0.023). A higher normal/reactive component was also observed in FLAIR-only area (mean: 29.00±37.15%, range: 10-95%) rather than CE (p=0.007), FLAIR+PET area (p=0.019) and

PET-only area (p=0.045). No significant differences were observed between the FLAIR-only area and the radiologically normal samples (p>0.05). (Figure 4e)

Microvascular Proliferation

A statistically significant correlation was observed between microvascular proliferation patterns and the different areas analyzed (p=0.045). Specifically, all samples taken from radiologically normal areas showed no microvascular proliferation (100%). In contrast, all samples taken from the CE area exhibited microvascular proliferation (focal 60% and diffuse 40%). Four samples from the FLAIR+PET area showed focal microvascular proliferation (80%), while one did not show microvascular proliferation (20%). Lastly, samples from PET-only and FLAIR-only areas showed diffuse microvascular proliferation in one case (20%), focal proliferation in one case (20%), and no proliferation in three cases (60%) (Figure 4f).

Correlation between the Sample Collection Area and the Intensity of Intraoperative Fluorophore Uptake

We observed a statistically significant correlation in the intensity of 5-ALA uptake across the different sample collection areas (p=0.015). Specifically, all samples collected in the FLAIR+PET area showed intense 5-ALA uptake (100%), while samples obtained from the CE and PET-only areas exhibited intense 5-ALA uptake in 80% of cases and faint 5-ALA uptake in 20%. In the FLAIR-only samples, 20% demonstrated intense 5-ALA uptake, 60% showed faint 5-ALA uptake, and 20% showed no 5-ALA uptake. Finally, in samples taken from radiologically normal areas, 60% exhibited no 5-ALA uptake, while 40% showed faint 5-ALA uptake (Figure 4g).

In addition, intraoperative SF uptake was significantly correlated with the different sample collection areas ($p<0.001$). All CE samples displayed intense SF uptake (100%), while 60% of PET-only samples showed intense SF uptake and 40% showed faint SF uptake. In the FLAIR+PET samples, 40% exhibited intense SF uptake, and 60% showed faint SF uptake. In the FLAIR-only samples, 60% showed no SF uptake, 40% exhibited faint SF uptake, and none showed intense SF uptake (0%). No samples obtained from radiologically normal areas displayed intraoperative SF uptake (Figure 4h). Interobserver agreement between the initial joint classification and the blinded evaluation was assessed using Cohen's kappa coefficient, showing excellent agreement for both 5-ALA ($\kappa = 0.933$) and sodium fluorescein ($\kappa = 0.819$).

DISCUSSION

In this interim analysis from the ongoing ResPGlioma study, we analyzed histopathological differences between samples taken from distinct brain regions identified by varying radiological features during preoperative evaluation. We also assessed whether these samples showed different uptake patterns of the intraoperative fluorophores 5-ALA and SF. The standard treatment for GB-IDH WT includes surgical resection followed by radiotherapy and temozolomide chemotherapy.[20] Despite this, median survival remains around 15–18 months, which can extend to 20–25 months when gross total resection (GTR) is achieved.[9] GTR is defined as the complete removal of the CE area seen on T1-weighted MRI after gadolinium administration[21]. However, complete resection is difficult due to gliomas' infiltrative nature, often spreading into surrounding brain tissue. MRI sensitivity is limited by tumor cell density, and tumor cells can be present even in radiologically normal-appearing brain areas, highlighting the risk of residual undetected tumor after surgery and the need for adjuvant therapies.[2,22] Previous studies show higher neoplastic cell density, mitotic

activity, and microvascular proliferation in CE regions compared to FLAIR-positive areas. CE regions typically represent the most aggressive tumor parts, with neoangiogenesis and blood-brain barrier disruption causing the pronounced MRI contrast enhancement.[23,24]

[^{18}F]-DOPA PET and histopatological correlation

Our results showed that samples from CE areas had significantly more necrosis than those from PET-only (p=0.020), FLAIR-only (p=0.004), and radiologically normal regions (p=0.018). Necrosis is a negative prognostic factor in GB, emphasizing the importance of complete CE resection.[25] However, neoplastic cells often remain in the peritumoral FLAIR region, contributing to recurrence despite adjuvant therapy. This has led to interest in the prognostic value of "FLAIRectomy.".[5,26,27] Li et al. showed that resecting more than 53% of the FLAIR hyperintense area beyond the CE zone correlates with improved survival.[28] Similarly, Pessina et al. reported favorable outcomes when at least 45% of the FLAIR region was resected. In contrast, other studies found no significant survival benefit associated with FLAIRectomy.[29]

Recently, the RANO resect group classified the extent of resection, demonstrating that, in patients with complete CE resection, removing more than 5 cm³ of non-CE tissue (class 1) was associated with improved survival.[1] However, in clinical practice, ensuring resection of >5 cm³ of non-CE tissue remains difficult, even with meticulous preoperative planning and neuronavigation. Extending resection beyond the CE area is limited by the presence of eloquent brain regions, where surgical injury could result in significant neurological deficits. Thus, the guiding surgical principle

in glioma management is “maximal safe resection,” aiming to remove the largest possible tumor volume without impairing neurological function. [30]

To overcome these limitations, some authors suggest using metabolic imaging like AA-PET to better identify surgically relevant peritumoral regions.[31,32] AA-PET more accurately defines tumor infiltration beyond the contrast-enhancing margin, distinguishes tumor tissue from vasogenic edema in FLAIR areas, and reveals tumor heterogeneity and aggressiveness.[11,12] In the present study patients underwent PET with [18F]DOPA. Different tracers ([^{11}C]Methionine, [^{18}F]-FET, [^{18}F]DOPA), all show similar accuracy for imaging in glioblastoma although there’s lack of studies directly comparing them, especially in the presurgical setting. [33,34]In this regard it should be noted that physiological striatal DOPA uptake is a potential challenge in the evaluation of lesions with basal ganglia involvement; however, several studies, including PET RANO recommendations, provided instructions to overcome this potential issue and DOPA PET in widely used for PET imaging in patients with gliomas. [35]

Our results show that biopsies from PET-only areas had significantly higher neoplastic cell density and mitotic activity compared to FLAIR-only areas ($p = 0.002$ and $p = 0.035$, respectively). No statistically significant differences were observed between PET-only and CE areas, nor between FLAIR-only and radiologically normal regions ($p > 0.005$). Additionally, FLAIR+PET samples displayed higher tumor cell density ($p = 0.002$) and mitoses ($p = 0.011$) compared to FLAIR-only areas, with no significant differences compared to CE regions.

These findings confirm that PET-positive regions, even outside the CE zone, are characterized by high tumor cell density. Particularly noteworthy is that within the FLAIR area, PET-positive zones showed a greater tumor burden than FLAIR-only areas. This supports the idea that PET imaging

can be a valuable tool for guiding more extensive resections, especially when FLAIRectomy is limited by proximity to eloquent cortex.[15] In this regard the concept of “PET-positive” regions might deserve a further discussion as we applied a thresholding based on SUVmean of the contralateral striatum while other thresholds such as T/N > 2 was reported in biopsy-controlled studies. [12,36] In this regard, while the threshold T/N > 2.0 is highly sensitive, in the specific context of IDH-wildtype glioblastoma, a more conservative threshold (such as one based on the striatum) may, at least in theory, better identify the "metabolic core" most relevant for supramaximal resection, reducing the risk of including healthy parenchyma in the surgical target. It is, however, worthwhile to note that, in the present study, the demonstration that BTV based on striatal SUVmean extended beyond the CE MRI margins in 100% of cases and the biopsies performed within these DOPA-positive/CE-negative areas consistently showed tumor infiltration and high proliferative activity (Ki-67). These results provide preliminary histological evidence that a striatal-based threshold might be also effective in identifying viable tumor tissue that is missed by conventional MRI.

Conversely, FLAIR-only biopsies showed greater infiltration of white matter compared to CE, FLAIR+PET, and PET-only samples ($p = 0.021$, $p = 0.037$, and $p = 0.042$, respectively), consistent with earlier observations by Broggi et al.[37]. Moreover, Altieri et al. demonstrated that FLAIR peritumoral regions can harbor tumor stem cells in concentrations comparable to those in CE areas, particularly in zones with similar intraoperative 5-ALA fluorescence[26].

[^{18}F]-DOPA PET and intraoperative fluorescence

Resection of PET-positive areas can be hindered by neuronavigation limitations, particularly brain shift, which affects the spatial accuracy of pre-incision coordinates. To improve targeting accuracy, adjunct techniques such as intraoperative fluorescence guidance have been proposed.[38,39] Müther et al. showed that 5-ALA-guided resection beyond the CE zone reduced postoperative 18F-FET PET uptake. [40]Similarly, Shimuzu et al. found a strong correlation between 5-ALA fluorescence and MeT-PET uptake.[41] Both 5-ALA and AA-PET reflect tumor metabolism and proliferation. Our results confirm that 5-ALA uptake and fluorescence intensity were higher in CE, FLAIR+PET, and PET-only areas compared to FLAIR-only and radiologically normal tissue ($p = 0.015$).

The relationship between intraoperative sodium SF uptake and AA-PET has been less thoroughly investigated. Schebesch et al. described five patients with non-enhancing gliomas that were FET-PET positive, in whom intraoperative fluorescence matched PET-positive areas, suggesting subtle blood–brain barrier disruption undetectable by gadolinium-enhanced MRI.[42] Our findings similarly showed greater SF uptake in CE and PET-positive regions compared to normal and FLAIR-only areas. Interestingly, 60% of FLAIR-only zones showed no uptake, whereas 60% of FLAIR+PET regions exhibited intense fluorescence.

Accessibility of Amino Acid PET

Despite the clear clinical benefit of 18F-DOPA PET in identifying non-enhancing tumor infiltration, its systematic implementation in the preoperative workup of newly diagnosed glioblastoma is often limited by practical and structural constraints. Recent data from the EORTC-Brain Tumour Group survey underscore that all amino acid PET availability remains heterogeneous across Europe.[43] Even in regions with established infrastructure, logistical hurdles

such as tracer production, reimbursement policies, and the narrow window for surgical intervention in symptomatic high-grade gliomas often preclude its use. In the relatively urgent setting of a newly diagnosed glioblastoma, the clinical necessity for immediate surgical decompression frequently outweighs the delay required to schedule a PET scan. Consequently, while our results demonstrate that 18F-DOPA PET could by a useful tool for achieving supramaximal resection, its current use is a restricted number of mainly tertiary or academic centers. Future strategies must focus on overcoming these 'real-world' barriers to ensure that precision-medicine approaches in neuro-oncology become accessible during the critical acute phase of the disease.

LIMITATIONS

This study has several limitations. First, although derived from a larger prospective cohort, the relatively small sample size included in this analysis reflects the application of stringent selection criteria. These criteria were necessary to ensure a homogeneous patient population and, most importantly, to guarantee the accuracy of biopsies. Furthermore, although tissue samples were collected prior to the start of tumor resection to minimize the effects of brain shift on neuronavigation, factors such as dural opening and cerebrospinal fluid drainage may have compromised the precision of sampling. Finally, the intensity of intraoperative uptake of 5-ALA and SF was assessed subjectively, albeit by two neurosurgeons and a blinded reviewer with experience in the use of intraoperative fluorescence. With respect to DOPA PET imaging PET RANO group recommended a visual plausibility check and manual correction to ensure that structures with physiologically high uptake (including the striatum in the case of [18F]DOPAPET) are not encompassed in the volume of interest. In our case, fused PET/MRI images have been also

used to optimize segmentation due to the vicinity with the basal ganglia and to minimize potential impact on the results of semiquantification. [44,45]

Finally, the threshold we used for BTV was defined based on the mean standard uptake value of the contralateral striatum which lacks the same level of extensive histological validation at present available to the tumor-background ratio[12,36]. Although the present results support the applicability of this choice (but do not allow inferring its performance with respect to other thresholds), the cut-off used for BTV definition might have a partial impact on the results of the study; therefore further studies are needed to more directly compare the added value of different thresholds used for BTV definition on AA-PET. In this regard it should be also noted that in 2023, a framework for standardized tissue sampling during resection in gliomas has been published by the RANO consortium. While the consortium further recommended the use of PET to support neuronavigation for the delineation of metabolic hotspots and to support BTV sampling, no specific indications were provided for the threshold for BTV definition. [46]

CONCLUSIONS

Our preliminary findings confirm that preoperative DOPA-PET imaging can help identify areas of significant tumor infiltration within the non–contrast-enhancing peritumoral zone, thereby enabling a safer and more effective supramarginal resection than approaches based solely on FLAIR sequences. The intraoperative fluorescence provided complementary insights: 5-ALA, as a metabolic fluorophore, showed strong correspondence with PET-positive areas, while FS confirmed its role as a blood-brain barrier disruption marker. Their use may facilitate the complete resection of PET-positive regions, while also reducing the impact of brain shift on neuronavigation accuracy.

Ethics: Ethical approval for this study (IRB n. 698050/2023) was obtained from the Institutional Review Board. All procedures performed were in accordance with the ethical standards of the institutional research committee and with the 1964 Helsinki declaration and its later amendments. Informed consent was obtained from all individual participants included in the study.

Funding: This research did not receive any funding

Acknowledgements: This study was conducted as part of the ResPGlioma study (NCT07567196), supported by the EANS Research Fund Award 2025. The present work predates the award and received no dedicated funding.

Disclosures: The authors have no personal, financial, or institutional interest in any of the drugs, materials, or devices described in this article.

Authorship: Conceptualization: A.B., F.C., S.M., D.G.; Methodology: A.B., L.B., F.C., P.C., G.M., R.R., S.M., D.G.; Investigation: A.B., A.P., R.D.M., M.Z., L.B., F.B., E.P., G.C., F.P., A.L.; Data curation: A.B., A.P., R.D.M., M.Z., L.B., F.B., E.P., G.C., F.P., A.L.; Formal analysis: A.P., R.D.M., M.Z., L.B., G.C.; Writing – Original draft preparation: A.B., A.P., R.D.M.; Writing – Review & Editing: A.B., A.P., M.Z., L.B., F.B., E.P., F.C., P.C., G.M., R.R., S.M., D.G.; Supervision: F.C., P.C., G.M., R.R., S.M., D.G.; Project administration: S.M., D.G.;

All authors reviewed and approved the final version of the manuscript and agree to be accountable for all aspects of the work.

Data Availability

The data supporting the findings of this study are available from the corresponding author upon reasonable request.

REFERENCES

1. Karschnia P, Young JS, Dono A, et al. Prognostic validation of a new classification system for extent of resection in glioblastoma: A report of the RANO resect group. *Neuro Oncol*. 2022;25(5):940. doi:10.1093/NEUONC/NOAC193
2. Angelucci C, D'Alessio A, Lama G, et al. Cancer stem cells from peritumoral tissue of glioblastoma multiforme: the possible missing link between tumor development and progression. *Oncotarget*. 2018;9(46):28116-28130. doi:10.18632/ONCOTARGET.25565
3. Cepeda S, Romero R, Luque L, et al. Deep learning-based postoperative glioblastoma segmentation and extent of resection evaluation: Development, external validation, and model comparison. *Neurooncol Adv*. 2024;6(1). doi:10.1093/NOAJNL/VDAE199
4. Altieri R, Barbagallo D, Certo F, et al. Peritumoral Microenvironment in High-Grade Gliomas: From FLAIRectomy to Microglia-Glioma Cross-Talk. *Brain Sci*. 2021;11(2):1-18. doi:10.3390/BRAINSCI11020200
5. Certo F, Altieri R, Maione M, et al. FLAIRectomy in Supramarginal Resection of Glioblastoma Correlates With Clinical Outcome and Survival Analysis: A Prospective,

Single Institution, Case Series. *Oper Neurosurg (Hagerstown)*. 2021;20(2):151-163. doi:10.1093/ONS/OPAA293

6. Pesaresi A, La Cava P, Bonada M, et al. Combined Fluorescence-Guided Surgery with 5-Aminolevulinic Acid and Fluorescein in Glioblastoma: Technical Description and Report of 100 Cases. *Cancers (Basel)*. 2024;16(16). doi:10.3390/CANCERS16162771
7. Senders JT, Muskens IS, Schnoor R, et al. Agents for fluorescence-guided glioma surgery: a systematic review of preclinical and clinical results. *Acta Neurochir (Wien)*. 2017;159(1):151-167. doi:10.1007/S00701-016-3028-5
8. Bianconi A, Bonada M, Zeppa P, et al. How Reliable Is Fluorescence-Guided Surgery in Low-Grade Gliomas? A Systematic Review Concerning Different Fluorophores. *Cancers (Basel)*. 2023;15(16). doi:10.3390/CANCERS15164130
9. Roh TH, Kim SH. Supramaximal Resection for Glioblastoma: Redefining the Extent of Resection Criteria and Its Impact on Survival. *Brain Tumor Res Treat*. 2023;11(3):166. doi:10.14791/BTRT.2023.0012
10. Wach J, Vychopen M, Kühnapfel A, Seidel C, Güresir E. A Systematic Review and Meta-Analysis of Supramarginal Resection versus Gross Total Resection in Glioblastoma: Can We Enhance Progression-Free Survival Time and Preserve Postoperative Safety? *Cancers (Basel)*. 2023;15(6). doi:10.3390/CANCERS15061772
11. Bauer EK, Stoffels G, Blau T, et al. Prediction of survival in patients with IDH-wildtype astrocytic gliomas using dynamic O-(2-[18F]-fluoroethyl)-L-tyrosine PET. *Eur J Nucl Med Mol Imaging*. 2020;47(6):1486-1495. doi:10.1007/S00259-020-04695-0
12. Pafundi DH, Laack NN, Youland RS, et al. Biopsy validation of 18F-DOPA PET and biodistribution in gliomas for neurosurgical planning and radiotherapy target delineation:

results of a prospective pilot study. *Neuro Oncol*. 2013;15(8):1058-1067. doi:10.1093/NEUONC/NOT002

13. Morana G, Piccardo A, Puntoni M, et al. Diagnostic and prognostic value of 18F-DOPA PET and 1H-MR spectroscopy in pediatric supratentorial infiltrative gliomas: a comparative study. *Neuro Oncol*. 2015;17(12):1637-1647. doi:10.1093/NEUONC/NOV099
14. FW F, D P, HJ W, et al. Multimodal metabolic imaging of cerebral gliomas: positron emission tomography with [18F]fluoroethyl-L-tyrosine and magnetic resonance spectroscopy. *J Neurosurg*. 2005;102(2):318-321. doi:10.3171/JNS.2005.102.2.0318
15. De Marco R, Pesaresi A, Bianconi A, et al. A Systematic Review of Amino Acid PET Imaging in Adult-Type High-Grade Glioma Surgery: A Neurosurgeon's Perspective. *Cancers (Basel)*. 2022;15(1). doi:10.3390/CANCERS15010090
16. Law I, Albert NL, Arbizu J, et al. Joint EANM/EANO/RANO practice guidelines/SNMMI procedure standards for imaging of gliomas using PET with radiolabelled amino acids and [18F]FDG: version 1.0. *Eur J Nucl Med Mol Imaging*. 2019;46(3):540-557. doi:10.1007/S00259-018-4207-9
17. Bertaux M, Berenbaum A, Di Stefano AL, et al. Hybrid [18F]-F-DOPA PET/MRI Interpretation Criteria and Scores for Glioma Follow-up After Radiotherapy. *Clin Neuroradiol*. 2022;32(3):735-747. doi:10.1007/S00062-022-01139-0
18. Garelli G, Rovera G, Levis M, et al. [18F]DOPA PET for lesion definition and contouring using different thresholds in patients with gliomas. *The quarterly journal of nuclear medicine and molecular imaging : official publication of the Italian Association of Nuclear Medicine (AIMN) [and] the International Association of Radiopharmacology*

(IAR), [and] Section of the Society of. 2024;68(3):200-206. doi:10.23736/S1824-4785.24.03587-8

19. Bianconi A, Bonada M, Zeppa P, et al. Double fluorescence-guided surgery with 5-ALA and fluorescein sodium in grade 2 and grade 3 adult-type diffuse gliomas: retrospective analysis of 112 cases. *Brain & spine*. 2025;5. doi:10.1016/J.BAS.2025.104277
20. Bianconi A, Koumantakis E, Gatto A, et al. Effects of Levetiracetam and Lacosamide on survival and seizure control in IDH-wild type glioblastoma during temozolomide plus radiation adjuvant therapy. *Brain & spine*. 2023;4. doi:10.1016/J.BAS.2023.102732
21. Roux A, Elia A, Hudelist B, et al. Prognostic significance of MRI contrast enhancement in newly diagnosed glioblastoma, IDH-wildtype according to WHO 2021 classification. *J Neurooncol*. 2024;169(2):445-455. doi:10.1007/S11060-024-04747-7
22. D'Alessio A, Proietti G, Sica G, Scicchitano BM. Pathological and Molecular Features of Glioblastoma and Its Peritumoral Tissue. *Cancers (Basel)*. 2019;11(4). doi:10.3390/CANCERS11040469
23. Kubben P, Wesseling P, Lammens M, et al. Correlation between contrast enhancement on intraoperative magnetic resonance imaging and histopathology in glioblastoma. *Surg Neurol Int.* 2012;3(1):158. doi:10.4103/2152-7806.105097
24. Barajas RF, Phillips JJ, Parvataneni R, et al. Regional variation in histopathologic features of tumor specimens from treatment-naive glioblastoma correlates with anatomic and physiologic MR Imaging. *Neuro Oncol*. 2012;14(7):942-954. doi:10.1093/NEUONC/NOS128

25. Raza SM, Lang FF, Aggarwal BB, et al. Necrosis and glioblastoma: a friend or a foe? A review and a hypothesis. *Neurosurgery*. 2002;51(1):2-13. doi:10.1097/00006123-200207000-00002

26. Altieri R, Broggi G, Certo F, et al. Anatomical distribution of cancer stem cells between enhancing nodule and FLAIR hyperintensity in supratentorial glioblastoma: time to recalibrate the surgical target? *Neurosurg Rev*. 2022;45(6):3709-3716. doi:10.1007/S10143-022-01863-8

27. Haddad AF, Young JS, Morshed RA, Berger MS. FLAIRectomy: Resecting beyond the Contrast Margin for Glioblastoma. *Brain Sci*. 2022;12(5):544. doi:10.3390/BRAINSCI12050544

28. Li YM, Suki D, Hess K, Sawaya R. The influence of maximum safe resection of glioblastoma on survival in 1229 patients: Can we do better than gross-total resection? *J Neurosurg*. 2016;124(4):977-988. doi:10.3171/2015.5.JNS142087

29. Pessina F, Navarria P, Cozzi L, et al. Maximize surgical resection beyond contrast-enhancing boundaries in newly diagnosed glioblastoma multiforme: is it useful and safe? A single institution retrospective experience. *J Neurooncol*. 2017;135(1):129-139. doi:10.1007/S11060-017-2559-9

30. Armocida D, Bianconi A, Zancana G, et al. DTI fiber-tracking parameters adjacent to gliomas: the role of tract irregularity value in operative planning, resection, and outcome. *J Neurooncol*. 2025;171(1):241-252. doi:10.1007/S11060-024-04848-3

31. Ort J, Hamou HA, Kernbach JM, et al. 18F-FET-PET-guided gross total resection improves overall survival in patients with WHO grade III/IV glioma: moving towards a

multimodal imaging-guided resection. *J Neurooncol*. 2021;155(1):71-80. doi:10.1007/S11060-021-03844-1

32. Harat M, Rakowska J, Harat M, et al. Combining amino acid PET and MRI imaging increases accuracy to define malignant areas in adult glioma. *Nat Commun*. 2023;14(1). doi:10.1038/S41467-023-39731-8

33. Galldiks N, Kaufmann TJ, Vollmuth P, et al. Challenges, limitations, and pitfalls of PET and advanced MRI in patients with brain tumors: A report of the PET/RANO group. *Neuro Oncol*. 2024;26(7):1181-1194. doi:10.1093/NEUONC/NOAE049

34. Somme F, Bender L, Namer IJ, Noël G, Bund C. Usefulness of 18F-FDOPA PET for the management of primary brain tumors: a systematic review of the literature. *Cancer Imaging*. 2020;20(1):1-13. doi:10.1186/S40644-020-00348-5

35. Albert NL, Galldiks N, Ellingson BM, et al. PET-based response assessment criteria for diffuse gliomas (PET RANO 1.0): a report of the RANO group. *Lancet Oncol*. 2024;25(1):e29-e41. doi:10.1016/S1470-2045(23)00525-9

36. Cicone F, Carideo L, Minniti G, Scopinaro F. The mean striatal 18F-DOPA uptake is not a reliable cut-off threshold for biological tumour volume definition of glioma. *Eur J Nucl Med Mol Imaging*. 2019;46(5):1051-1053. doi:10.1007/S00259-019-4276-4

37. Broggi G, Altieri R, Barresi V, et al. Histologic Definition of Enhancing Core and FLAIR Hyperintensity Region of Glioblastoma, IDH-Wild Type: A Clinico-Pathologic Study on a Single-Institution Series. *Brain Sci*. 2023;13(2). doi:10.3390/BRAINSCI13020248

38. Orillac C, Stummer W, Orringer DA. Fluorescence Guidance and Intraoperative Adjuvants to Maximize Extent of Resection. *Neurosurgery*. 2021;89(5):727-736. doi:10.1093/NEUROS/NYAA475

39. Stummer W, Stepp H, Wiestler OD, Pichlmeier U. Randomized, Prospective Double-Blinded Study Comparing 3 Different Doses of 5-Aminolevulinic Acid for Fluorescence-Guided Resections of Malignant Gliomas. *Neurosurgery*. 2017;81(2):230-239. doi:10.1093/NEUROS/NYX074

40. Müther M, Koch R, Weckesser M, Sporns P, Schwindt W, Stummer W. 5-Aminolevulinic Acid Fluorescence-Guided Resection of 18F-FET-PET Positive Tumor Beyond Gadolinium Enhancing Tumor Improves Survival in Glioblastoma. *Neurosurgery*. 2019;85(6):E1020-E1029. doi:10.1093/NEUROS/NYZ199

41. Shimizu K, Tamura K, Hara S, et al. Correlation of Intraoperative 5-ALA-Induced Fluorescence Intensity and Preoperative 11C-Methionine PET Uptake in Glioma Surgery. *Cancers (Basel)*. 2022;14(6). doi:10.3390/CANCERS14061449

42. Schebesch KM, Brawanski A, Doenitz C, et al. Fluorescence-guidance in non-Gadolinium enhancing, but FET-PET positive gliomas. *Clin Neurol Neurosurg*. 2018;172:177-182. doi:10.1016/J.CLINEURO.2018.07.011

43. Mair MJ, Lohmann P, Galldiks N, et al. Availability and use of PET in patients with brain tumours - a European Organisation for Research and Treatment of Cancer - Brain Tumour Group (EORTC-BTG) survey. *Eur J Nucl Med Mol Imaging*. 2025;52(12):4627-4638. doi:10.1007/S00259-025-07366-0

44. Albert NL, Preusser M. Measure what is measurable: PET RANO 1.0 criteria for interpretation of amino acid PET of diffuse gliomas. *Neuro Oncol*. 2024;26(3):401-402. doi:10.1093/NEUONC/NOAD228

45. Müller KJ, Forbrig R, Reis J, et al. Measurable disease as baseline criterion for response assessment in glioblastoma: A comparison of PET -based (PET RANO 1.0) and MRI-

based (RANO) assessments. *Neuro Oncol*. 2025;27(1):77-88. doi:10.1093/NEUONC/NOAE208

46. Karschnia P, Smits M, Reifenberger G, et al. A framework for standardised tissue sampling and processing during resection of diffuse intracranial glioma: joint recommendations from four RANO groups. *Lancet Oncol*. 2023;24(11):e438-e450. doi:10.1016/S1470-2045(23)00453-9

Figure captions:

Figure 1: flow chart of patient selection criteria and study protocol

Figure 2: Example of patient 1 showing tumor volumes and biopsy sites. a) axial MRI T1w CE; b) axial MRI FLAIR c) axial 18F-DOPA PET; d) axial T1w CE and five biopsy sites: CE) CE area; FP) FLAIR+PET area; Po) PET-only area; Fo) FLAIR-only area; N) area with no evident PET/MRI disease. Different tumor volumes are described as: Yellow: FLAIR volume; Blue: PET volume; Red: CE volume)

Figure 3: Representative histopathological images of the different samples: contrast-enhancing and PET-positive (A), contrast-enhancing only (B), PET-positive only (C) and MRI T2/FLAIR-positive only without contrast-enhancement or PET-positivity (D). A: HE image shows a high-grade glial neoplasm with high cellularity, brisk mitotic activity and presence of microvascular proliferations. Necrosis was also present in other sample areas. These features, integrated by molecular profiling, are consistent with a glioblastoma, IDH-wildtype diagnosis. B and C:

histological findings are similar to figure A and enable the diagnosis of glioblastoma, IDH-wildtype. D: conversely, in this sample, a moderate increase of cellularity and focal mitotic activity were present, consistent with a tumor infiltration/histologically lower-grade area.

Figure 4a-f: Analysis of correlation between the collected samples and histopathological features: a) Neoplastic Component; b) Necrotic Component; c) Mitoses; d)Infiltrative Component; e)Normal/Reactive Component; f) Microvascular Proliferation. The Mann Whitney U test was used. *, $p < 0.05$. Figure 4g-h: Intraoperative fluorescence intensity across different tumor and peritumoral regions.g) 5-ALA fluorescence and h) fluorescein sodium fluorescence for five patients. Each column corresponds to one patient, and each row represents a different biopsy sampling area: contrast-enhancing tumor (CE), FLAIR+PET overlap (FP), PET-only region (Po), FLAIR-only region (Fo), and radiologically normal tissue (N). The fluorescence intensity is color-coded according to the legend: intense and faint fluorescence are shown in darker and lighter shades respectively, while grey indicates no fluorescence. The chi-square (χ^2) test was used. *, $p < 0.05$.

Table 1: Demographic, clinical and tumor characteristics of the study population

Table 2: Histopathological characteristics as previously described in the five biopsy sites

Lay Summary

Glioblastoma is an aggressive brain tumor with a high likelihood of regrowth even after surgery, as tumor cells often spread beyond the visible edges seen on standard MRI scans. In this study, we used a special brain scan called [^{18}F]DOPA PET before surgery to identify hidden areas of active tumor. By analyzing tissue samples from these areas, we confirmed that PET-positive regions contain high concentrations of tumor cells, similar to the main tumor mass. These same areas also glowed under fluorescent light during surgery, helping surgeons remove them more precisely. Our findings suggest that combining PET imaging with fluorescence-guided surgery could enable safer, more complete tumor removal and potentially improve outcomes for patients.

Table 1

	Patient 1	Patient 2	Patient 3	Patient 4	Patient 5	Mean ± SD
Gender	Female	Female	Male	Male	Female	-
Age (years)	56	65	71	70	66	68.4 ± 8.8
Preoperative KPS	100	90	80	90	100	92 ± 4.5
Location	Temporal	Temporal	Frontal	Frontal	Frontal	-
CE Volume (cm^3)	11.5	1.55	44.6	30.3	15.1	20.6 ± 16.9
PET Volume (cm^3)	33.6	4.73	47.1	44.8	21.6	30.4 ± 17.6
FLAIR Volume (cm^3)	31.2	5.35	59.4	165.4	39.1	60.1 ± 62.0

Table 2

	CE	FP	Po	Fo	N
Neoplastic Component (%)	92.00±8.37	82.00±24.90	78.00±27.75	21.00±17.46	9.00±17.46
Necrotic Component (%)	25.00±13.23	11.00±13.42	6.00±6.52	1.00±2.24	6.00±5.48
Mitoses (/10HPF)	22.60±14.64	18.40±8.14	22.80±19.52	5.20±3.90	1.60±2.07
Infiltrative Component (%)	8.00±8.37	16.00±20.74	18.00±19.24	54.00±35.07	22.00±25.88
Normal/Reactive Component (%)	0.00±0.00	2.00±4.47	4.00±8.94	29.00±37.15	63.00±44.10

Microvascular Proliferations					
Absent	0/5 (0%)	1/5 (20%)	3/5 (60%)	3/5 (60%)	5/5 (100%)
Focal	3/5 (60%)	4/5 (80%)	1/5 (20%)	1/5 (20%)	0/5 (0%)
Diffuse	2/5 (40%)	0/5 (0%)	1/5 (20%)	1/5 (20%)	0/5 (0%)

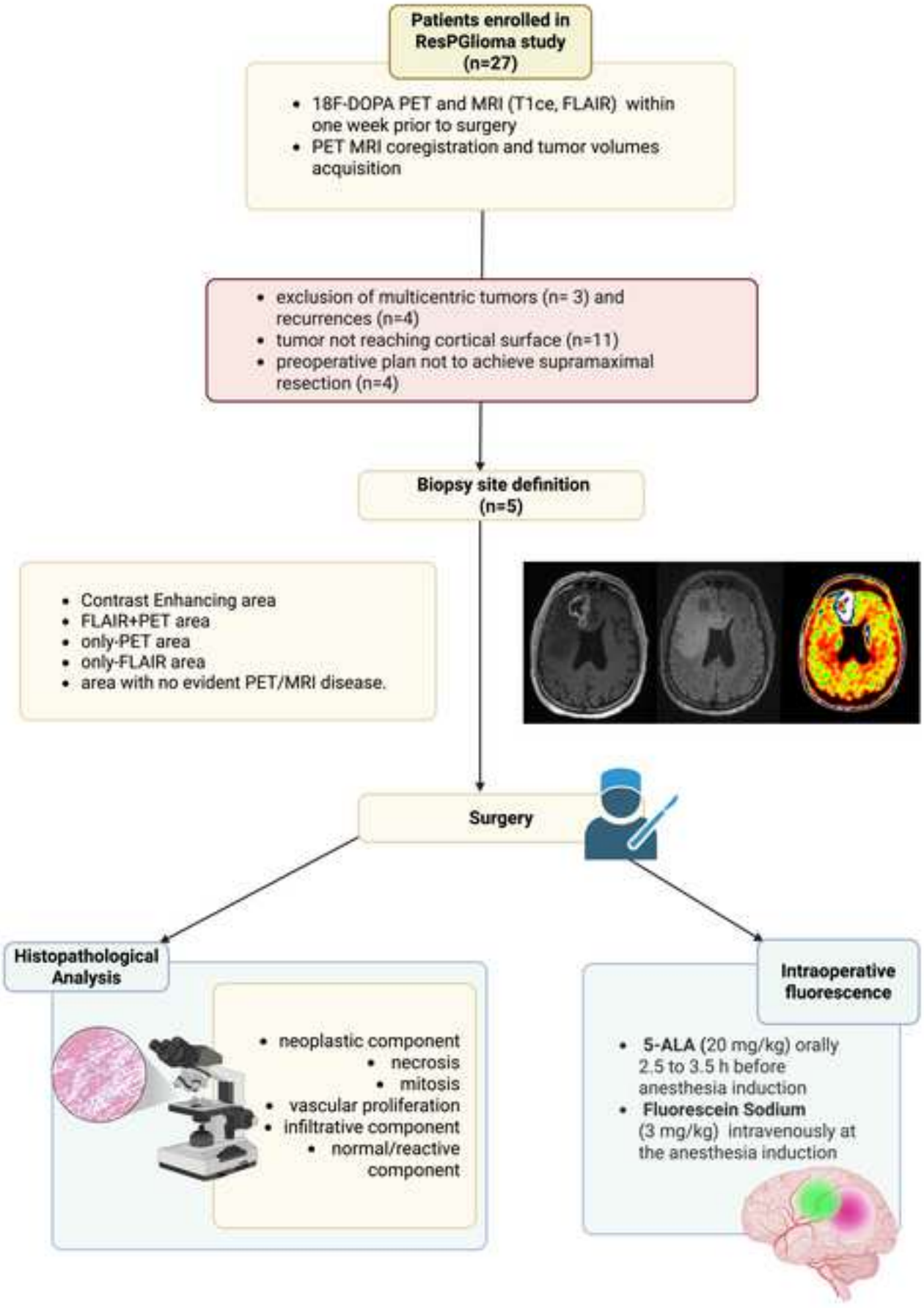

Figure 2

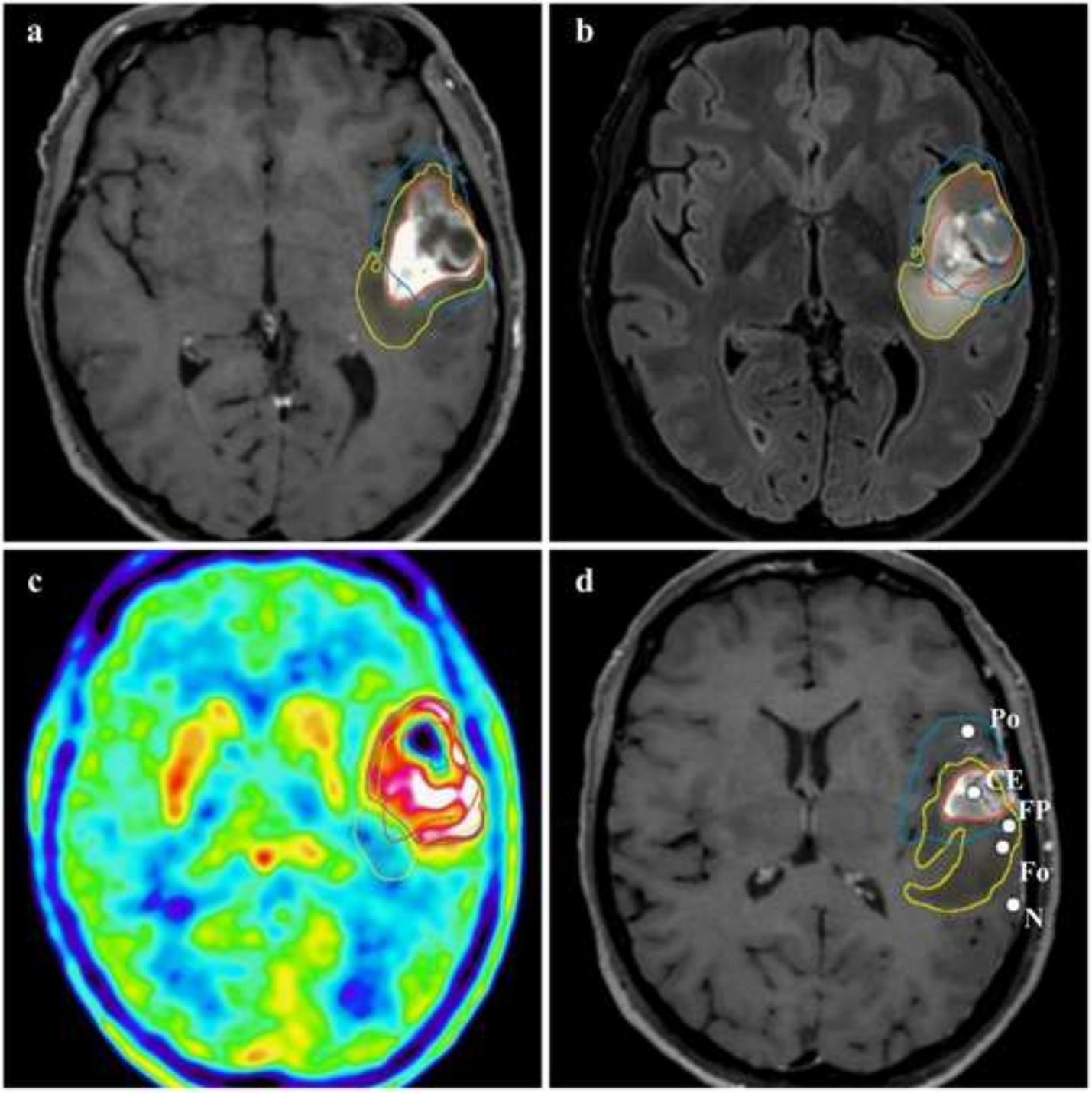

Figure 3

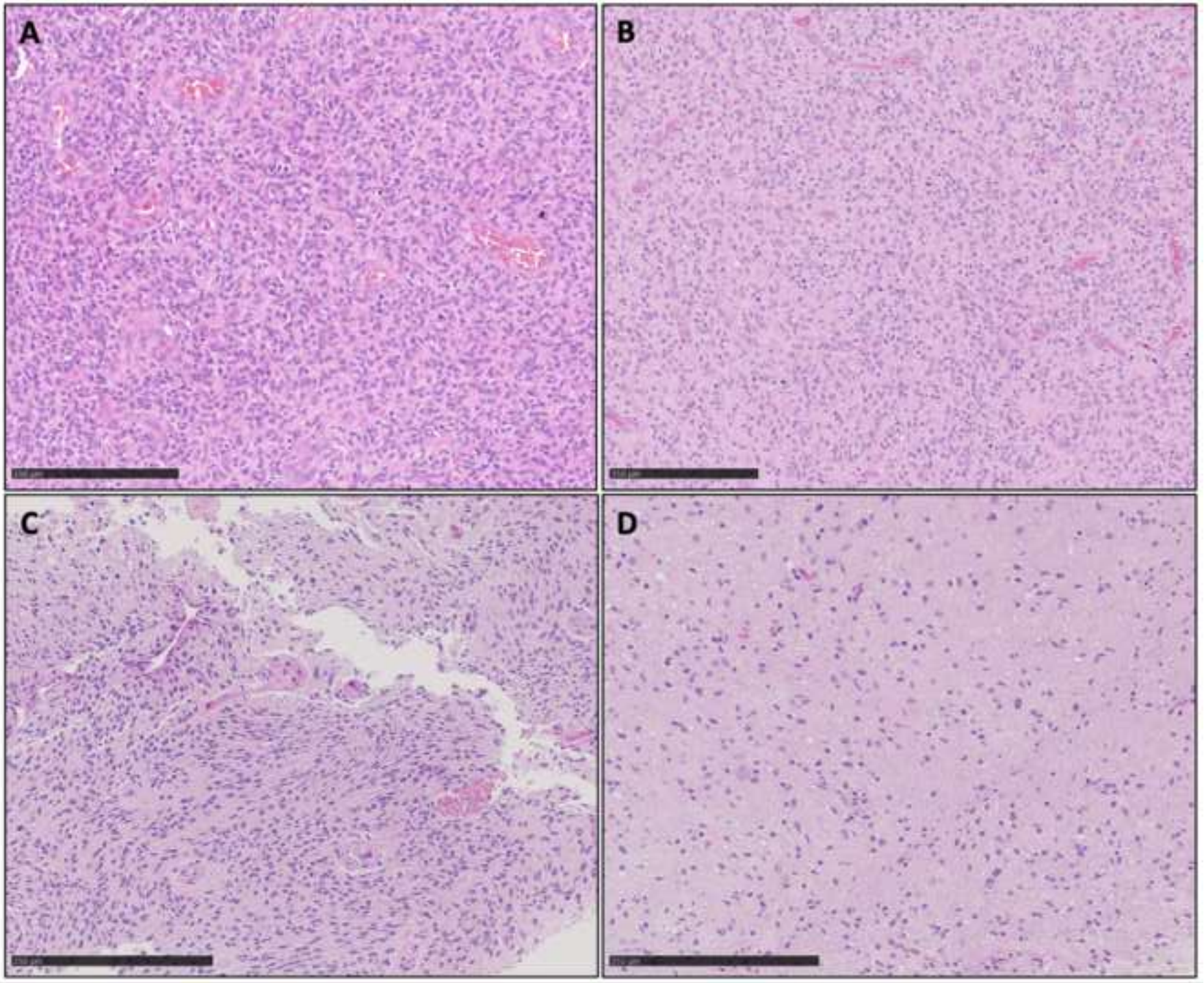

Figure 4